PHYSICOCHEMICAL PROPERTIES OF MnO-BASED SLAGS FOR THE PRODUCTION OF MANGANESE FERROALLOYS

Joo Hyun Park

Department of Materials Engineering, Hanyang University, Ansan 426-791, Korea
e-mail: basicity@hanyang.ac.kr

ABSTRACT

The physicochemical properties of MnO-based slags are highly important in operation efficiency and product quality of manganese ferroalloys. Because the thermophysical properties of slags such as viscosity, electrical conductivity, and density significantly affect the process efficiency, the fundamental understanding of these properties based on the structure of molten silicates is necessitated. Thus, we investigated the structure of molten MnO-CaO-SiO_2 slag using micro-Raman spectroscopy and found linear correlations between thermophysical properties and a degree of polymerization of the slag. The viscosity and the activation energy for viscous flow of the slag linearly increased with increasing degree of polymerization, whereas density and electrical conductivity linearly decreased as a degree of polymerization of silicate melts increased. The addition of CaF_2 in the MnO-CaO-SiO_2 slag decreased the viscosity of slags containing as high as about 10%MnO which is relatively close to SiMn slag. However, the addition of CaF_2 in the 40%MnO system, which is close to FeMn slag, does not change the viscosity. This indicates that MnO is very effective network-modifier, which was confirmed by structure analysis using Raman spectroscopic method. The sulfur absorption capability, i.e. sulfide capacity of MnO-CaO-SiO_2-Al_2O_3-MgO slags was also measured by gas-slag equilibration method. The sulfide capacity increases with increasing MnO content at a fixed CaO/SiO_2 ratio and increases as MnO substitutes for CaO at a fixed SiO_2 content. The addition of Al_2O_3 and MgO does not significantly change the sulfide capacity of MnO-based slag. All these phenomena could be understood based on structure analysis using Raman spectroscopic methodology.

KEYWORDS: *MnO-based slags, viscosity, electrical conductivity, density, silicate structure, raman spectroscopy, degree of polymerization, sulfide capacity.*

1. INTRODUCTION

Even though there have been several studies on the physicochemical properties of the CaO–SiO_2–MnO slag due to its importance in smelting and refining processes for the production of manganese ferroalloys, the systematic and fundamental approach on the structure of this slag system is scarcely found. Jung et al. [1] measured the relative content of three types of oxygens such as bridging (O^0), non-bridging (O^-), and free oxygen (O^{2-}) in the CaO–SiO_2–MnO system by X–ray photoelectron spectroscopy (XPS) and found that the silicate melts were depolymerized by addition of MnO at a fixed CaO/SiO_2 ratio.

The slag-metal reaction kinetics should be enhanced in view of high production rate and low cost in smelting and refining processes of Mn-ferroalloys. In order to meet these requirements, it is necessary to consider and quantify the effect of fluorspar (CaF_2) addition on the viscosity of MnO-containing slags at high temperatures, because the CaF_2 is well known to decrease the viscosity of silicate melts. Even though the experimental study of the effect of CaF_2 on the viscosity of various silicate melts has been investigated by several researchers for CaO-SiO_2 (-MgO)-CaF_2 [2], FeO(-CaO)-SiO_2-CaF_2 [3], CaO-SiO_2-Na_2O-Li_2O-CaF_2 [4], and CaO-Al_2O_3-SiO_2-MgO-CaF_2 systems [5],

the effect of CaF_2 on the viscosity of MnO-based slags is still not known yet.

Additionally, the demand for Mn-ferroalloys has increased continuously due to the introduction of advanced high strength steels such as TRIP and TWIP aided steels that were recently developed to contain Mn up to about 30 %. Thus, the removal of impurity such as sulfur from Mn-ferroalloys is an important issue. Even though many researchers have investigated the sulfide capacities of molten slags, there are few experimental data regarding high MnO–containing multicomponent slags. Nzotta et al. [6] measured the sulfide capacities of the $CaO–SiO_2–MnO–Al_2O_3–MgO$ slags and found that the sulfide capacity of the slags dominantly increased by increasing the MnO content. Also, the sulfide capacity of the $CaO–SiO_2–MnO–MgO$ slags were strongly decreased by increasing the silica content and moderately decreased with increasing MgO/CaO ratio at given silica and alumina contents [7].

From these previous works, the quantitative information on the structure and viscosity of the $CaO–SiO_2–MnO$ ($–CaF_2$) slags and the sulfide capacity of the $CaO–SiO_2–MnO–Al_2O_3–MgO$ slags are still highly necessitated. Consequently, in the present study, firstly, the effects of CaO/SiO_2 ratio and Ca↔Mn substitution on the silicate structure of the $CaO–SiO_2–MnO$ slag are investigated by employing Raman spectroscopic analysis. Furthermore, the relationships among the structural information, thermophysical properties such as viscosity, density and electrical conductivity are developed. Secondly, the effect of CaF_2 addition on the viscosity of the $CaO-SiO_2-MnO$ slag was measured by rotating cylinder method and the structure of slags was analyzed using Raman spectroscopy. Finally, the effect of MnO content and Ca↔Mn substitution on sulfide capacity of the slags was systematically investigated.

2. EXPERIMENTAL

2.1. Structure Analysis of $CaO-SiO_2-MnO$ ($-CaF_2$) Slags

The reagent grade MnO, CaF_2 and SiO_2 powder (99.9 % purity) was used in the present study. The CaO was obtained from the reagent grade $CaCO_3$ (99.9 % purity) calcined at 1273 K during 10 hours. Powders of CaO, SiO_2, MnO and CaF_2 were weighted to get the required composition and mixed for 1 hour to obtain homogeneous mixtures. The mixture was melted in a Pt crucible at 1873 K during 2 hours for homogenization and for bubble–free liquid under purified Ar atmosphere. Here the Ar gas was highly purified by passing the gas through the silica gel and a furnace containing magnesium turnings at 723 K.

After 2 hours, the crucible was quickly drawn from the furnace and the melt was rapidly quenched by pouring it on to a copper mold in the cooling water. The whole samples were confirmed to be glassy state by XRD pattern. The compositions of glass samples were determined with an XRF. Raman spectra of the present glass samples were collected at room temperature in the range 100–1900 cm^{-1} using an Ar excitation laser source having wavelength 514.5 nm coupled with Jobin–Yvon Horiba micro–Raman spectrometer. Raman shifts were measured with a precision of 0.3 cm^{-1} and the spectra resolution was of the order 1 cm^{-1}. The quantitative peak deconvolution was carried out through the range of Raman shifts from 800 to 1200 cm^{-1}. The spectrum data were fitted by Gausssian function with an aid of the 'PeakFit' program within ±0.5% error limit and thus the relative abundance of the Q^n (n=0, 1, 2, 3) units was calculated from the area fraction of the best–fitted Gaussian curves at the frequency for the symmetric stretching vibration of each Q^n unit.

2.2. Viscosity Measurements of $CaO-SiO_2-MnO-CaF_2$ Slags

The rotating cylinder method was used in the present study and a schematic diagram of the experimental apparatus is shown in figure 1. A rotating viscometer was set on the super kanthal

electric furnace. The temperature was measured using an R-type thermocouple. The experimental temperature range was about 1523 to 1873 K. The measurements of viscosity in the present study were made using a Pt-10%Rh alloy spindle, crucibles, and suspending wire. The experiment was started by placing the crucible, containing pre-melted slag, inside the reaction chamber at 1873 K. Then, the spindle rotating at a speed of 100 rpm was lowered into the slag. The tip of the bob was placed about 5 mm above the base of the crucible and about 5 mm of the shaft was immersed in the melt.

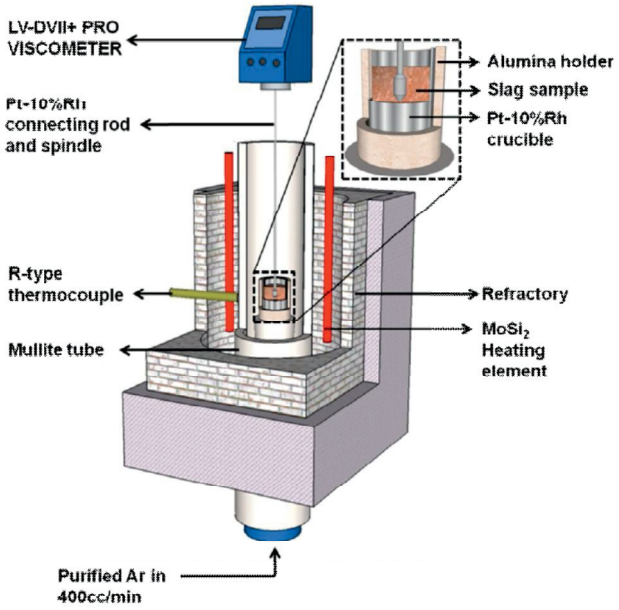

Figure 1: Experimental apparatus for the measurement of slag viscosity

The equilibration time was approximately 20 minutes at each temperature. Standard oil samples with viscosity of 0.0486, 0.0952, 0.50 and 0.985 Pa·s (0.486, 0.952, 5.0 and 9.85 poise) were used to calibrate the spindle. In addition, the CaF_2 content of the slag samples was analyzed using XRF after experiments, because evaporation of the fluoride species from the melts was expected. It was confirmed that the weight loss of CaF_2 by fluoride emission during viscosity measurements was within about 5 % of the initial content. Hence, the composition in the present article refers to initial content.

2.3. Measurements of Sulfide Capacity of the CaO-SiO_2-MnO-Al_2O_3-MgO Slags

A kanthal super vertical electric resistance furnace was used for equilibration between the CaO–SiO_2–MnO–Al_2O_3–MgO slag and gas phase at 1873 K. A slag sample of 1.2 g was maintained in a Pt crucible, which was held in a porous alumina holder under the CO–CO_2–SO_2–Ar gas mixture for 8 hours. The flow rate of each gas and the calculated oxygen and sulfur potentials are listed in table 1. The schematic diagram of the experimental apparatus is shown in figure 2.

Table 1: Mass flow of each gas and calculated oxygen and sulfur partial pressures

Mass flow of gas phases (ml/min)					Gas potential (atm)	
CO	**CO_2**	**SO_2**	**Ar**	**Total**	p_{O_2}	p_{S_2}
125	160	15	100	400	2.80×10^{-7}	4.71×10^{-3}

After equilibration, each sample was quickly drawn from the furnace and then quenched by dipping it into brine. The quenched samples were crushed to less than 100 μm using stainless steel and agate mortars for chemical analysis. The contents of sulfur and each component in the slag were determined by a combustion analyzer and XRF, respectively.

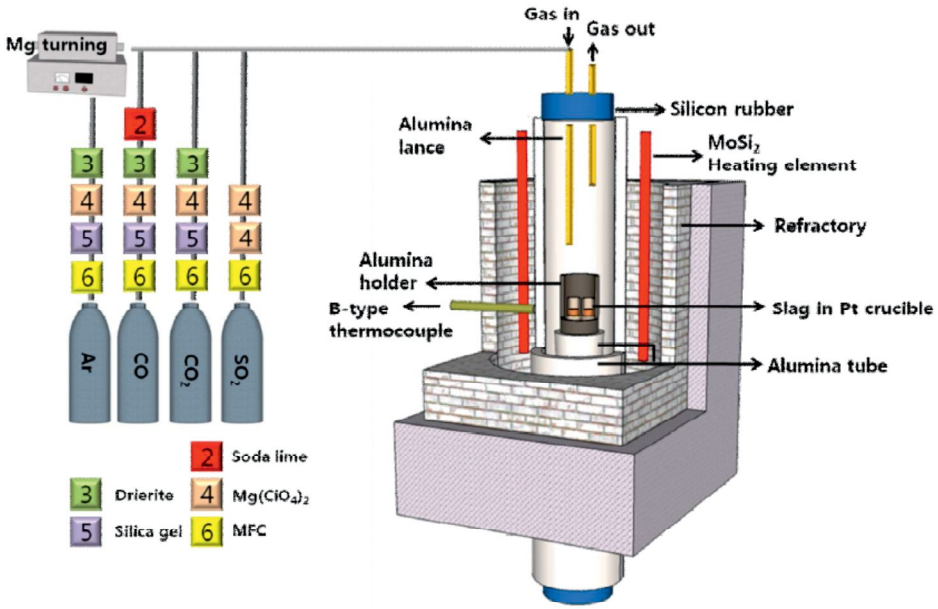

Figure 2: Experimental apparatus for the measurement of sulfide capacity of slags

3. RESULTS AND DISCCUSION

3.1. Structure-Property Relationship of CaO-SiO_2-MnO Slags

The Raman spectra of the CaO–MnO–50%SiO_2 system as a function of wavenumbers range from 700 to 1300 cm^{-1} are shown in figure 3. The main silicate envelope is definitely resolved to Q^0 (860(±5) cm^{-1}) and Q^2 (960(±5) cm^{-1}) bands in the CaO–SiO_2 binary system, while there is a broad asymmetric band between 960 and 1050 cm^{-1} at Mn/(Mn+Ca)=0.76 [8]. Even though it is not easy to find a conclusive variation of Raman spectra with one's eye as MnO substitutes for CaO, a broadening of Raman band qualitatively suggests that the substitution of CaO by MnO made a stronger perturbation and hence a more depolymerized configuration of local environment of Q–species in high MnO melts at a fixed silica content [9]. However, the more quantitative analysis can be given by the deconvolution of Raman spectra as follows.

The relative fractions of the silicate anionic units obtained from a Gaussian deconvolution of Raman bands are also plotted against Mn/(Mn+Ca) ratio in figure 3. The fraction of Q^2 unit increases and that of Q^3 unit decreases with increasing Mn/(Mn+Ca) ratio. The fractions of Q^0 and Q^1 units slightly decrease but not significant with increasing Mn/(Mn+Ca) ratio. Therefore, the Q^3/Q^2 ratio, viz. degree of polymerization decreases by increasing the Mn/(Mn+Ca) ratio based on the following equation:

$$[Si_2O_5]^{2-}(Q^3) + (O^{2-}) = 2[SiO_3]^{2-}(2Q^2) \quad (1)$$

The free oxygen in Eq. [1] is supplied from a dissociation of MnO as shown in Eq. (2) in the relatively high MnO region.

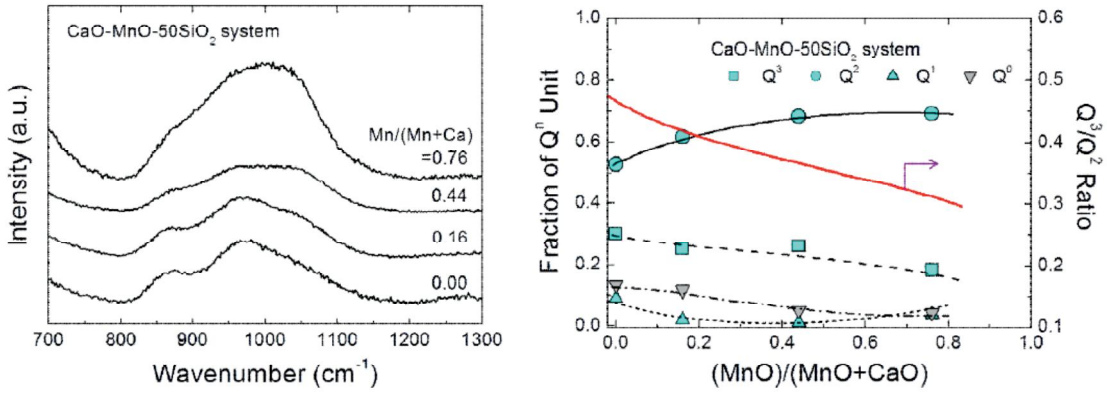

Figure 3: (a) Raman spectra and (b) abundance of structural units and Q^3/Q^2 ratio in the CaO–MnO–50%SiO_2 system with Mn/(Mn+Ca)=0~0.8

$$(MnO) = Mn^{2+} + O^{2-} \quad (2)$$

The network–modifying role of MnO in this composition range can be discussed as follows. From an analysis of McMillan [9], doubly–charged cations M^{2+} of large ionic radius, i.e. small ionization potential (= Z/r^2) should preferentially occupy the more open, coupled Q^3 ($\equiv Si–O^-)_2$ sites, while smaller M^{2+} cations with larger ionization potential will favor the higher charge concentration offered by the Q^2 (=$Si–2O^-$) sites. This is schematically expressed in figure 4. Because the ionization potential of Ca^{2+} (Z/r^2=2) is lower than that of Mn^{2+} (Z/r^2=2.4~3.0 according to electron spin) [10] the Ca^{2+} ion is charge balanced with two open O^- ions due to its large [CaO_6] cage, whereas the Mn^{2+} ion is balanced with two adjacent corner–shared O^- ions due to its small [MnO_6] cage as shown in figure 4.

Hence, as the Mn^{2+} ions substitute for Ca^{2+} ions, the Ca^{2+} ions are balanced with two open O^- ions via weak ionic bond due to their network–modifying role, whereas the abundant Mn^{2+} ions are not only balanced with two corner–shared O^- ions but also partly free from a network–modifying role. The latter Mn^{2+} ions can stabilize the S^{2-} ions when they are exposed to appropriate sulfur potential, which will be discussed in later section in further detail.

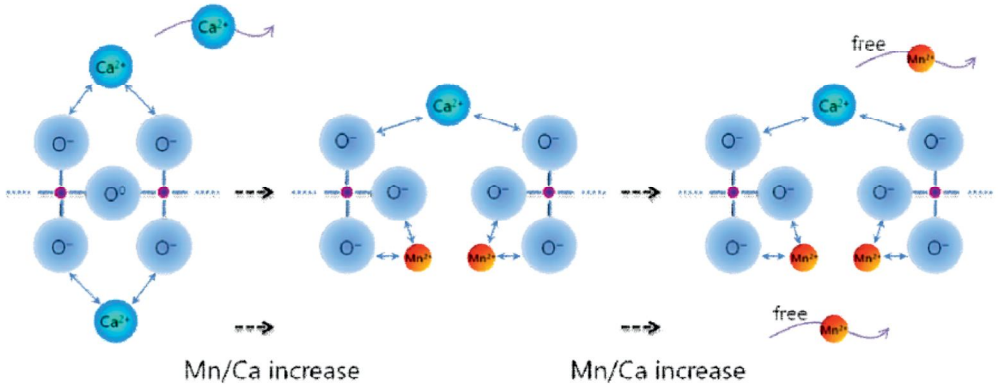

Figure 4: Schematics of the structural modification by Ca^{2+} and Mn^{2+} ions in the 50 % SiO_2 system

As discussed above, because the Q^3/Q^2 ratio is defined as a polymerization index in the present study, the viscosity of the CaO–MnO–SiO_2 system at 1873 and 1773 K is plotted against the

Q^3/Q^2 ratio in a logarithmic form in figure 5. The viscosity of the silicate melts, ln η, linearly increases by increasing the ln (Q^3/Q^2) at 1873 and 1773 K. The activation energy for the viscous flow of silicate melts in a Newtonian flow region above the liquidus temperature is also shown in figure 5 as a function of ln (Q^3/Q^2). The activation energy of silicate melts was obtained from an Arrhenius relationship (eq. 3) between viscosity and temperature.

$$\eta = \eta_o \exp\left(\frac{E_\eta}{RT}\right) \tag{3}$$

In figure 5, the activation energy for the viscous flow of CaO–MnO–SiO_2 slag is a linear function of degree of polymerization which is defined as ln (Q^3/Q^2) in the present study as follows.

$$E_\eta(\text{kJ}) = 17.6(\pm 2.7)\cdot \ln\frac{Q^3}{Q^2} + 162.7(\pm 4.3) \quad (r^2=0.85) \tag{4}$$

Consequently, the ln (Q^3/Q^2) is believed as a good polymerization index, which can be experimentally obtained, to quantify the effect of silicate structure on the viscosity of silicate melts.

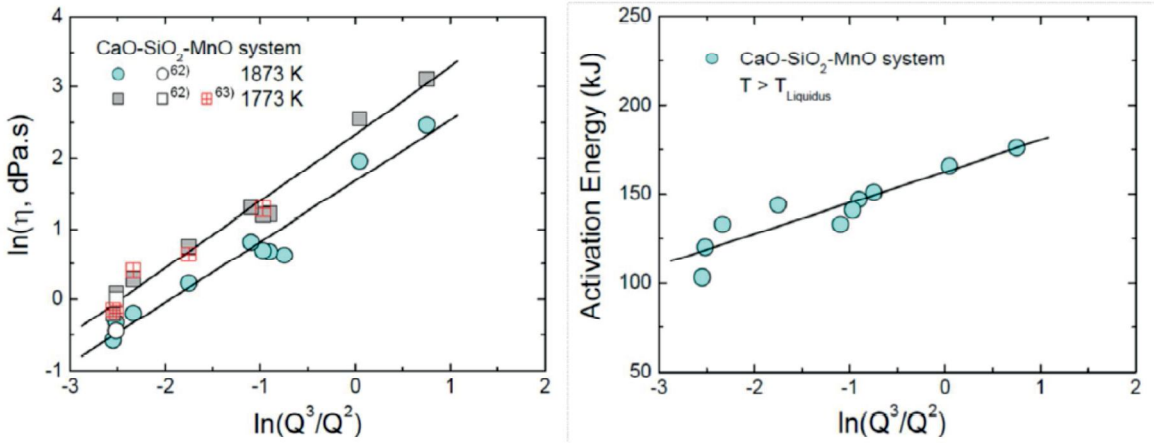

Figure 5: Viscosity (a) and activation energy (b) as a function of Q^3/Q^2 in the CaOa functi$_2$ slag

The relationship between density of the CaO–MnO–SiO_2 slag at 1773 and 1873 K and ln (Q^3/Q^2) value is shown in figure 6. Even though there are not so much experimental data for the present system, a density of melts linearly decreases by increasing the ln (Q^3/Q^2). From a fact that the molar volume of pure liquid silica had a tendency of becoming smaller when network–modifying oxides are dissolved in pure SiO_2 in spite of their larger partial molar volume than that of SiO_2, Bottinga and Richet concluded that the bridging oxygens have a larger partial molar volume than non-bridging oxygens [11]. Consequently, the present result shown in Figure 6 is consistently on the line of theoretical consideration.

The relationship between the electrical conductivity (ln κ) and a degree of polymerization, viz. ln (Q^3/Q^2) of the CaO–MnO–SiO_2 slag at 1773 K is also shown in Figure 6, wherein the ln κ linearly decreases by increasing the ln (Q^3/Q^2) with the following correlations that was obtained from a least square regression analysis.

$$\ln \kappa\ (\Omega^{-1}.cm^{-1}) = -0.69(\pm 0.09) \cdot \ln \frac{Q^3}{Q^2} - 1.89(\pm 0.17)\ \ (r^2=0.94) \qquad (5)$$

Bockris et al. [12] concluded from their experimental results and the absolute reaction rate theory that the conductance due to O^{2-} ions was improbable and a decrease in the activation energy with increase of network–modifying oxides originated from the fact that the breakdown of silicates facilitated cationic transport. Hence, the present result shown in figure 6 is in good accordance to the Bockris et al.'s electrical conductance mechanism.

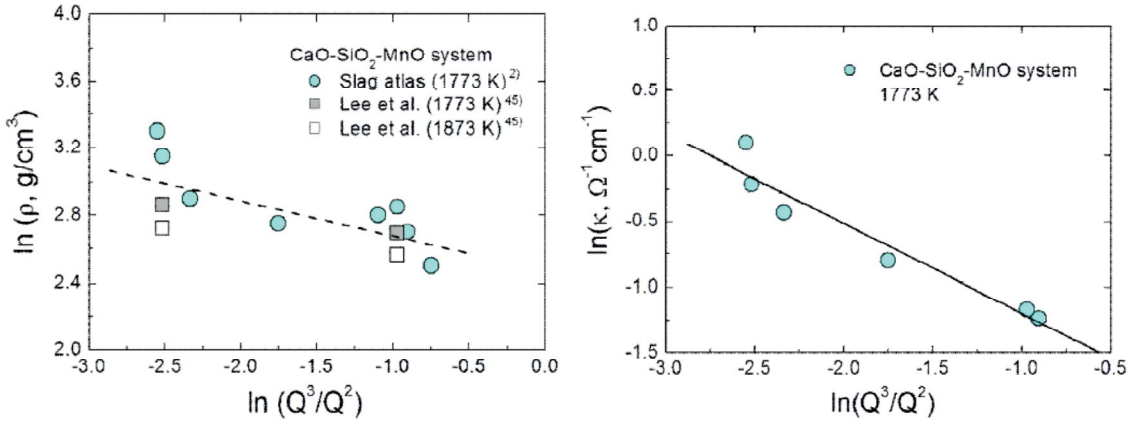

Figure 6: Density (a) and electrical conductivity (b) as a function of Q^3/Q^2 in $CaO–MnO–SiO_2$ slag

3.2. Effect of CaF_2 Addition on the Viscosity of $CaO-SiO_2-MnO$ (C/S=1.0) Slags

A temperature dependency of the viscosity for the 10 and 40% MnO systems are compared in figure 7 at different CaF_2 contents. The critical temperature (T_{CR}) of 10% MnO system decreases from about 1623 to 1543 K as the content of CaF_2 increases from 0 to 10% (figures 7(a)-(c)), followed by a rebound to about 1623 K when the CaF_2 content reaches 15% (figure 7(d)). For the 40% MnO system, there is no significant change in critical temperature (1673(±5) K) when the CaF_2 content varies from 0 to 10% (figures 7(a)-(c)). However, it abruptly increases to about 1723 K when the CaF_2 content changes from 10 to 15% (figure 7(d)).

Furthermore, in figure 7, the effect of MnO content on the viscosity of slags at temperatures greater than T_{CR} increases by decreasing the content of CaF_2. This means that MnO is also relatively strong network modifier as likely as CaO in the CaF_2-free silicate melts. The structural role of Ca^{2+} and Mn^{2+} ions in a depolymerization process of the $CaO-SiO_2-MnO$ ternary system was systematically discussed in figures 3 and 4.

The Arrhenius plot (eq. 3) for the $CaO-SiO_2-MnO-CaF_2$ slags is shown in figure 8 as a function of 1/T and the contents of MnO and CaF_2, respectively. The viscosity, ln η of the melts linearly increases with increasing 1/T and the viscosity of the 40% MnO system is unambiguously lower than that of 10% MnO system at given temperature and CaF_2 content. The slope of the line decreases with increasing CaF_2 content in 10% MnO system, whereas it is less discernible against CaF_2 content in 40% MnO system. This means that F^- ions effectively contributed to the depolymerization of silicate networks in the former, but not in the latter.

The activation energy for the viscous flow of silicate melts is also plotted against the content of CaF_2 in various fluorosilicate systems in figure 8.

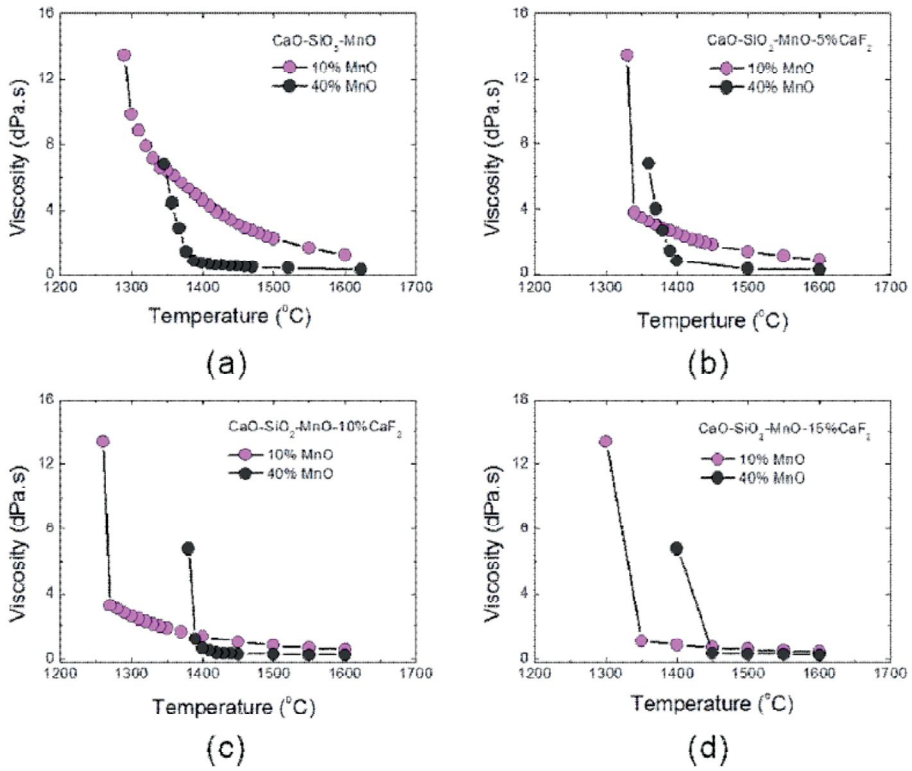

(a) CaF_2-free, (b) 5%, (c) 10%, (d) 15% CaF_2

Figure 7: Effect of CaF_2 and MnO content on the viscosities of the $CaO\text{-}SiO_2\text{-}MnO\text{-}CaF_2$ (C/S=1.0) slags

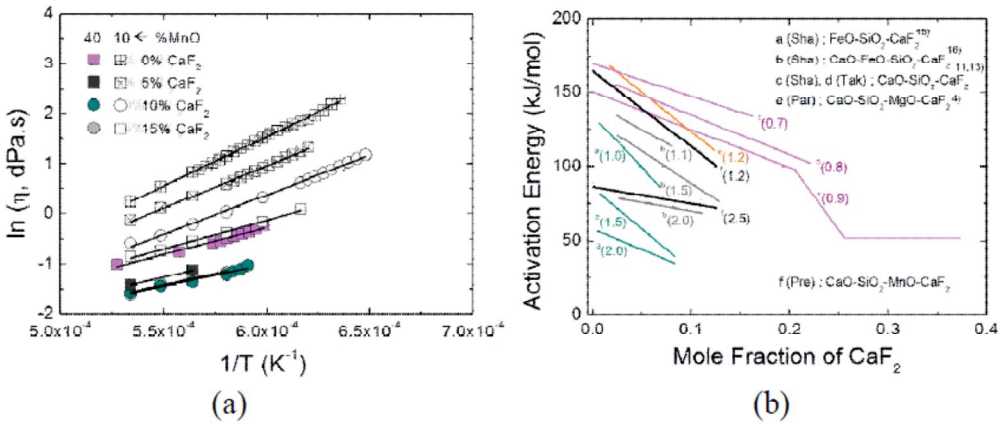

Figure 8: (a) Arrhenius plot and (b) the activation energy for the viscous flow of $CaO\text{-}SiO_2\text{-}MnO\text{-}CaF_2$ (C/S=1.0, CaF_2=0~15%) slags

One can find that the activation energy ranges from about 40 to 170 kJ/mol according to slag systems and commonly decreases with increasing content of CaF_2 regardless of slag systems. Also, the effect of CaF_2 on the activation energy becomes less significant as the basicity (B=(CaO+FeO+MnO+MgO)/SiO_2) increases. This is not only because the dominant fractions of silicates are depolymerized into the simpler forms such as $[SiO_4]$-tetrahedrons and/or $[Si_2O_7]$-dimers due to network-modifying role of Ca^{2+}, Fe^{2+}, Mn^{2+} and Mg^{2+} ions before F^- ions are working but also because the absolute amounts of silicates should be broken to flow are reduced as the

basicity increases.

3.3. Sulfide Capacity of the CaO-SiO_2-MnO-Al_2O_3-MgO Slags

The effect of MnO content on the sulfide capacity of the CaO–SiO_2–MnO(–Al_2O_3–MgO) slags at 1873 K is shown in figure 9. The sulfide capacity increases with increasing MnO content, indicating that MnO behaves as a basic oxide in the present slag system. Also, the higher the Vee ratio (B=CaO/SiO_2=C/S), the greater the capacity is obtained at a given MnO content. It is interesting that the sulfide capacity of the ternary and quinary slags are not so much different at the similar C/S condition [13,14]. The sulfide capacity of the CaO–SiO_2–MnO(–Al_2O_3–MgO) slags at 1873 K is also plotted in figure 9 against the activity of MnO in a logarithmic scale. Based on a definition of sulfide capacity, eq. [7], it is expected to be proportional to the activity of O^{2-} ion in a logarithmic scale as indicated in eq. [8] assuming that the activity coefficient of S^{2-} ion is not significantly affected by slag composition.

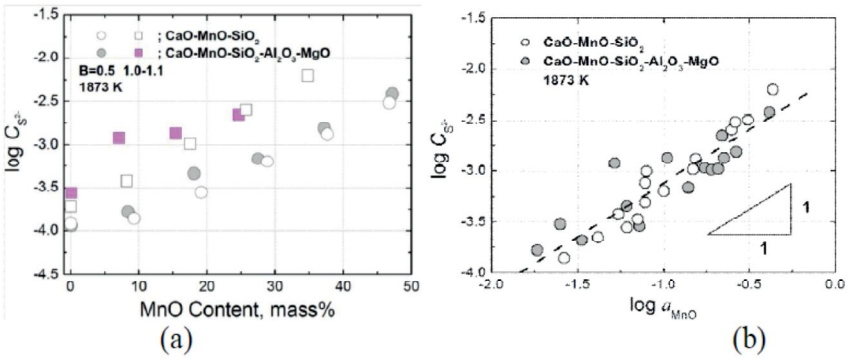

Figure 9: Effect of a) MnO content and b) MnO activity on the sulfide capacity of CaO-SiO_2-MnO (-Al_2O_3-MgO) slags at 1873 K

$$\frac{1}{2}S_2(g) + (O^{2-}) = (S^{2-}) + \frac{1}{2}O_2(g) \tag{6}$$

$$C_{S^{2-}} \equiv \frac{K_{[6]} \cdot a_{O^{2-}}}{f_{S^{2-}}} = (\text{wt\%S}) \cdot \left(\frac{p_{O_2}}{p_{S_2}} \right)^{0.5} \tag{7}$$

$$\log C_{S^{2-}} = \log a_{O^{2-}} - \log f_{S^{2-}} + \log K_{[6]} \tag{8}$$

where $K_{[6]}$ is the equilibrium constant of eq. [6], $a_{O^{2-}}$ is the activity of O^{2-} ion, and $f_{S^{2-}}$ is the Henrian activity coefficient of S^{2-} ion in the slag. However, due to thermodynamic restriction, the activity of basic oxide is assumed to be proportional to that of O^{2-} ion based on eqs. [2] and [9].

$$\log a_{MnO} = \log a_{O^{2-}} + \log a_{Mn^{2+}} - \log K_{[2]} \tag{9}$$

By combining eqs. (8) and (9), the following relationship can be deduced.

$$\log C_{S^{2-}} = \log a_{MnO} - \log a_{Mn^{2+}} - \log f_{S^{2-}} + C \tag{10}$$

where C may be assumed less sensitive to slag composition. As shown in figure 3, there is a linear correlation between $\log C_{S^{2-}}$ and $\log a_{MnO}$ with the following equation (obtained from a linear regression analysis):

$$\log C_{S^{2-}} = 1.05(\pm 0.08) \cdot \log a_{MnO} - 2.06(\pm 0.09) \quad (r^2=0.85) \tag{11}$$

Therefore, it is thermodynamically concluded that MnO is dominantly affect the sulfur dissolution behaviour in Ca–Mn–silicate melts.

4. CONCLUSIONS

Because the thermophysical properties of MnO-based slags such as viscosity, electrical conductivity, and density significantly affect the process efficiency, the fundamental understanding of these properties based on the structure of molten silicates is necessitated. Thus, we investigated the structure of molten MnO-CaO-SiO_2 slag using micro-Raman spectroscopy and found linear correlations between thermophysical properties and a degree of polymerization of the slag. The viscosity and the activation energy for viscous flow of the slag linearly increased with increasing degree of polymerization, whereas density and electrical conductivity linearly decreased as a degree of polymerization of silicate melts increased.

The addition of CaF_2 in the MnO-CaO-SiO_2 slag decreased the viscosity of slags containing as high as about 10%MnO which is relatively close to SiMn slag. However, the addition of CaF_2 in the 40 % MnO system, which is close to FeMn slag, does not change the viscosity. This indicates that MnO is very effective network-modifier, which was confirmed by structure analysis using Raman spectroscopic method. The sulfide capacity of MnO-CaO-SiO_2-Al_2O_3-MgO slags was also measured by gas-slag equilibration method. The sulfide capacity increases with increasing MnO content at a fixed CaO/SiO_2 ratio and increases as MnO substitutes for CaO at a fixed SiO_2 content. The addition of Al_2O_3 and MgO does not significantly change the sulfide capacity of MnO-based slag. All these phenomena could be understood based on structure analysis using Raman spectroscopic methodology.

5. REFERENCES

[1] E.J. Jung, W. Kim, I. Sohn, and D.J. Min: J. Mater. Sci., 2010, vol. 45, pp. 2023-29.
[2] J.H. Park and D.J. Min: J. Non-Cryst. Solids, 2004, vol. 337, pp. 150-56.
[3] F. Shahbazian: Scand. J. Metall., 2001, vol. 30, pp. 302-08.
[4] H.S. Park, H. Kim, and I. Sohn: Metall. Mater. Trans. B, 2011, vol. 42B, pp. 324-30.
[5] L. Wu, J. Gran and Du Sichen: Metall. Mater. Trans. B, 2011, vol. 42B, pp. 928-31.
[6] M.M. Nzotta, Du Sichen and S. Seetharaman: ISIJ Int., 1998, vol. 38, pp. 1170-79.
[7] M.M. Nzotta: High Temp. Mater. Process., 1997, vol. 16, pp. 261-71.
[8] J.H. Park: ISIJ Int., 2012, vol. 52, pp. 1627-36.
[9] P. McMillan: Am. Mineral., 1984, vol. 69, pp. 645-59.
[10] R.D. Shannon: Acta Crystallogr. A, 1976, vol. 32A, pp. 751-926.
[11] Y. Bottinga and P. Richet: Geochim. Cosmochim. Acta, 1995, vol. 59, pp. 2725-31.
[12] J.O'M. Bockris, J.A. Kitchener, S. Ignatowicz, and J.W. Tomlinson: Trans. Faraday. Soc., 1952, vol. 48, pp. 75-91.
[13] G.H. Park, Y.B. Kang and J.H. Park: ISIJ Int., 2011, vol. 51, pp. 1375-82.
[14] J.H. Park and G.H. Park: ISIJ Int., 2012, vol. 52, pp. 764-69.